Continental Shelf Research 286 (2025) 105409

Contents lists available at ScienceDirect

Continental Shelf Research

journal homepage: www.elsevier.com/locate/csr

Circulation in Cross Sound, Alaska

Emily Lemagie [a,*], Christopher Paternostro [b], Phyllis J. Stabeno [a], Mark Zimmermann [c]

[a] NOAA Pacific Marine Environmental Laboratory, 7600 Sand Point Way NE, Seattle, WA, 98115-0070, USA
[b] NOAA Center for Operational Oceanographic Products and Services, 1305 East-West, Bldg. SSMC4, USA
[c] NOAA Alaska Fisheries Science Center, 7600 Sand Point Way NE, Seattle, WA, 98115-0070, USA

A B S T R A C T

Cross Sound is located in southeast Alaska's Alexander Archipelago and extends ~50 km eastward from the Gulf of Alaska to Icy Strait. Between May and August 2010, ten moorings were deployed at the entrances to Cross Sound and at key internal locations within the Sound. Instruments on each mooring measured current velocity and temperature; some also measured salinity. The tidal range in this region is large (>5 m), causing high current speeds (peak speed measured at 263 cm s^{-1}), with a strong fortnightly signal. The flow predominantly follows the bathymetry westward from Icy Strait through Cross Sound and into the Gulf of Alaska. Moorings captured an estuarine exchange with outflow near the surface and inflow at depth. Earlier multi-year moorings demonstrated that synoptic variability in water properties is greater in spring and fall than over the summer season. In summer, during spring tides, the water column can mix to the bottom, delivering nutrients into the surface euphotic zone. When spring tides coincided with a strong wind event, bottom temperatures increased by > 1 °C over 3 days.

1. Introduction

The Alexander Archipelago in Southeast Alaska is a region of high mountains, fjords, embayments, and complex bathymetry (Fig. 1). Cross Sound, which is connected by the Yakobi Sea Valley (>200 m deep) to the slope, is the northernmost entrance to the Inside Passage. Current speeds as large as 450 cm s^{-1} occur in these passageways (Hooge and Hooge, 2002). Due to topographic steering by the high mountains and large across-shore pressure gradients, offshore-directed gap winds are commonly funneled through Cross Sound, particularly during the cold season (Loescher et al., 2006; Ladd and Cheng, 2016). Daily-averaged wind speeds can exceed 10 m s^{-1} and extend >200 km offshore. Gap winds impact eddy formation and ocean circulation over the shelf and offshore waters and may contribute to primary productivity by entraining additional nitrate into the surface mixed-layer (Ladd and Cheng, 2016).

Cross Sound is an important area for both fisheries and tourism (Dugan et al., 2007). Tidal friction vertically mixes the water column, providing nutrients to the surface euphotic zone. Summer nutrients and long days support a rich ecosystem from primary production through fishes, marine mammals, and birds (Weingartner et al., 2009). Cruise ships, fishing vessels, and the Alaskan marine highway ferries navigate their way among the many islands, straits, and subsurface sea-mounds of the Sound.

Our study region primarily consists of four regions: the entrance to Cross Sound from the Gulf of Alaska, the north and south passages around the Inian Islands, the entrance to Glacier Bay, and Icy Strait (Fig. 1). Glacier Bay extends northward over 60 km, encompassing dozens of glaciers tucked into the mountain valleys (e.g. Hall et al., 1995). Two hundred years ago, the area of Glacier Bay was covered by a single glacier (Connor et al., 2009). The retreat of this glacier deposited a moraine outside the Bay resulting in a sill that is < 20 m deep at places, separating the deep waters of Icy Strait from those of Cross Sound. The entrance to Cross Sound includes a deep (>300 m) channel between Cape Bingham to the south and Cape Spencer to the north, with a shallower outcropping along the Cape Spencer side. Inside of Cross Sound, the channel is divided by the Inian Islands. North Inian Pass is the deeper channel (~300 m), while South Inian Pass is shallower (<100 m). To the south and east of the Inian Islands is a shallow moraine from the glacier that occupied what would become Glacier Bay. This moraine extends about half way across the strait towards Chichagof Island, creating a substantial blockage of water flow between Cross Sound and Icy Strait. Icy Strait is the northern part of a deep (>300 m) channel (Chatham Strait) that originates ~220 km to the south. This complex bathymetry plays an important role in defining the currents in the region.

Freshwater discharge into Cross Sound, Glacier Bay, and Icy Strait contributes to seasonal and spatial variability in salinity and stratification. Freshwater discharge is divided almost equally between lower elevation small watersheds and larger point sources, and between snowmelt and precipitation (Hill et al., 2009). Snowmelt is primarily related to temperature and elevation, with a peak in spring (low

* Corresponding author.
E-mail address: emily.lemagie@noaa.gov (E. Lemagie).

https://doi.org/10.1016/j.csr.2025.105409
Received 13 December 2023; Received in revised form 13 December 2024; Accepted 16 January 2025
Available online 18 January 2025

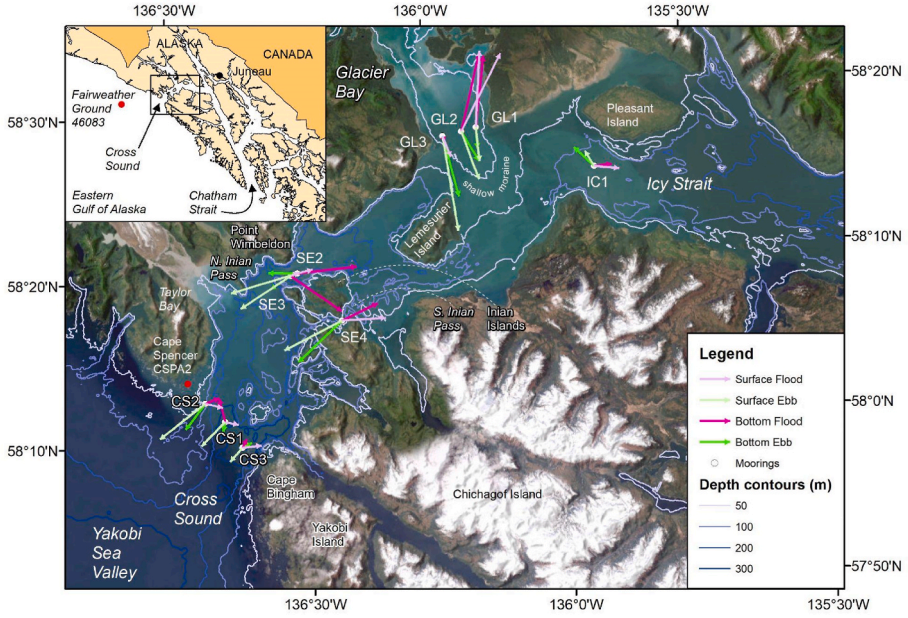

Fig. 1. Map of the Cross Sound region with local bathymetry and mooring locations, and mean ebb (green) and flood (purple) currents from near surface (light shading) and near bottom (dark shading) at each site using the ADCP data. (For interpretation of the references to color in this figure legend, the reader is referred to the Web version of this article.)

watersheds) or summer (high elevation watersheds), while maximum precipitation historically occurs in the autumn. The net result over this region is a broad distribution in peak seasonal discharge from May through October (Hill et al., 2009). Climate projections suggest a 13% increase in mean annual runoff and a potential seasonal shift towards a more rainfall dominated climate and towards maximum discharge occurring in fall (Crumley et al., 2019). Salinity variability measured offshore is weaker relative to the entrance to Cross Sound (Stabeno et al., 2016b) and the variability observed at the mouth is likely due to mixing between inland and offshore waters. Inside Glacier Bay, a surface lens of cold, relatively fresh water forms in summer, leading to the formation of a front north of the entrance sill that remains well mixed by the strong tides (Etherington et al., 2004). Strong tidal mixing also contributes to full water column mixing throughout the year over the shallow moraine from South Inian Pass, along the eastern side of North Inian Pass, and at the mouth of Glacier Bay (Hill et al., 2009). In Icy Strait, stratification is strongest in summer; surface temperatures warm rapidly by ~5 °C from lowest seasonal values in May and the surface freshens due to glacial and snow melt (Park et al., 2004).

The regional winds are influenced by the steep mountainous topography around Cross Sound. At Cape Spencer, wind directions are rotated relative to offshore and align with the Cross Sound channel. Wind forcing in this region is weakest and most variable in the spring and summer (Stabeno et al., 2016b). Winds were not the dominant driver of current variability. Other than a weak but significant correlation ($R^2 = 0.3$) between the alongshore wind speed and the mean transport at the mouth of Cross Sound, winds were not correlated with either surface or bottom currents over the study area.

The tidally forced flow is dominated by a strong M_2 tide (see details in Stabeno et al., 2016b). Many stations exhibit a dominant fortnightly signal in the low-pass filtered time series. This phenomenon has been observed throughout the region including the Aleutian Passes (Reed and Stabeno, 1993; Stabeno et al., 2005) and Kennedy Entrance (Stabeno et al., 2004). This fortnightly signal is the result of the nonlinear interaction of the large M_2 and S_2 tidal constituents exhibited in this region. The combination of these two constituents creates multiple compound tides. The nonlinear effects in this high velocity environment produce the high frequency overtides (M_4 and M_6) at significant amplitudes (Halverson, 2014). The strength of these overtides modulates with the phase of the combined M_2-S_2 frequency whose synodic period is about 14.8 days. Thus, the low frequency variation of the strengths of M_4 and M_6 over a period of 14.8 days accounts for the pulsating amplitudes in many of the stations and is captured in the lunisolar synodic fortnightly constituent, MSf.

There have been limited observations of bottom water properties and currents in Cross Sound. For instance, the annual predictions published in NOAA's Tidal Current Tables (https://tidesandcurrents.noaa.gov) were derived from observations collected in and before 1908. In 2010 a series of moorings were deployed to measure currents in the region and to update NOAA's Tidal Current Tables (Fig. 1). These measurements provide a more recent baseline of the area's tidal energy as well as of the general circulation of Cross Sound. As Alaska is experiencing accelerated physical and biological changes, these observations provide a baseline for comparison to future measurements. Stabeno et al. (2016b) examined the currents and stratification from five mooring stations over the coastal shelf and compared them to the currents and near-bottom water properties at the mouth of Cross Sound. Stabeno et al. (2016b) concluded that strong mixing within Cross Sound entrains nutrients to the surface waters, which flow onto the shelf around Icy Point and into locally formed eddies, contributing to primary productivity throughout the summer. This investigation of ten inland moorings provides additional insight into the mixing and transport of water between Cross Sound, Glacier Bay, and Icy Strait.

Moorings deployed during the summer of 2010 measured the currents and near-bottom temperature and salinity at ten locations in Cross Sound, Glacier Bay, and Icy Strait over 90 days. The seasonal mean and tidal variability of currents, temperature, and salinity over the summer–in each region–are explored, followed by a discussion of the spatial patterns. Additional moorings deployed at the three stations spanning the mouth of Cross Sound in the fall of 2005 and from the fall of 2006 through spring 2007 also provide a comparison among seasons. Direct comparisons of interannual variability over the summer at the locations across the mouth of Cross Sound and over the shelf are also available from mooring deployments made in 2011 and 2013 as part of the Gulf of Alaska Integrated Ecosystem Research Program (GOAIERP; Stabeno et al., 2016b).

Table 1
List of the moorings, deployment location, water depth and maximum velocity, mean and variance. Standard deviations are calculated relative to the variation in each parameter throughout the depth of the water column. Angles in degrees clockwise from North which is 0°.

Mooring (water depth)	Lat (°N) Lon (°W)	Dates Start End	Max Speed (cm s^{-1}) and Direction (°)	Mean Angle Ebb (°) Flood +180 (°)	Mean Speed ±Std. Dev. Ebb (cm s^{-1}) Flood (cm s^{-1})
CS1 (315 m)	58.149	5/21/10	134.4	211.6 ± 13	31.0 ± 7
	136.58	8/20/10	91°	211.8 ± 40	33.0 ± 16
CS2 (95 m)	58.174	5/21/10	161.8	228.3 ± 5	54.3 ± 9
	136.616	8/20/10	221°	268.6 ± 11	19.9 ± 1
CS3 (319 m)	58.119	5/21/10	127.2	171.1 ± 54	17.4 ± 5
	136.555	8/20/10	351°	233.6 ± 27	16.5 ± 3
GL1 (63 m)	58.382	5/20/10	253.3	172.5 ± 1	34.2 ± 5
	135.946	8/19/10	91°	186.6 ± 2	90.8 ± 2
GL2 (69 m)	58.382	5/20/10	263.2	155.4 ± 3	54.7 ± 6
	135.977	8/19/10	66°	200.2 ± 4	102.5 ± 3
GL3 (58 m)	58.383	5/20/10	238.7	168.6 ± 2	97.0 ± 12
	136.016	8/19/10	279°	161.1 ± 2[a]	18.9 ± 6
IC1 (134 m)	58.310	5/19/10	138.2	320.0 ± 6	23.4 ± 6
	135.738	8/20/10	26°	270.5 ± 5	30.4 ± 5
SE2 (292 m)	58.284	5/20/10	186.7	260.1 ± 6	61.4 ± 12
	136.370	8/19/10	9°	252.1 ± 5	53.0 ± 19
SE3 (296 m)	58.283	5/20/10	257.7	237.4 ± 2	60.0 ± 16
	136.385	8/19/10	113°	273.4 ± 16	46.1 ± 20
SE4 (67 m)	58.224	5/21/10	204.4	235.4 ± 5	74.4 ± 1
	136.308	8/19/10	208°	260.2 ± 7	51.9 ± 2

[a] Mean angle of flood not rotated by 180°, as in other columns.

2. Data and methods

2.1. Moorings

Ten current meter moorings were deployed for three months from mid-May to mid-August of 2010 (Table 1). Currents were measured using upward-looking, bottom-mounted 300 or 75 KHz (Teledyne RD Instruments) acoustic Doppler current profilers (ADCP). Specifically, to capture the complexities of the flow throughout Cross Sound, an array of three moorings was deployed across the mouth of Cross Sound and a second array of three moorings was deployed across the mouth of Glacier Bay (Fig. 1). Four other current meters were deployed at key locations in the Sound.

Two types of taut-line subsurface moorings were used dependent upon station depth. Shallow water moorings were deployed when water depths did not exceed 100 m. These stations had a 300 kHz ADCP at ~8 m off the bottom encased in a buoy to maintain stability in the water column. These shallow data were collected at 6 min intervals and hourly means were used in this analysis to align with water property measurements. At deeper stations, a 75 kHz ADCP current meter was deployed at ~20 m off the bottom encased in a spherical float. These instruments measured the current speed, current direction, and temperature analyzed at half-hourly intervals. At the five deeper moorings (CS1, CS3, IC1, SE2, SE3; Fig. 1), a SBE-37 was deployed below the ADCP to measure temperature and conductivity (salinity) at hourly intervals. All instruments were calibrated prior to deployment and the data were processed according to manufacturers' specifications.

2.2. Transport

Transports were calculated at the mouth of Cross Sound, Glacier Bay, and through Inian Pass. The calculations of transport follow methods described previously (Schumacher et al., 1989; Stabeno et al., 1995, 2016a). Briefly, the component of velocity normal to the line spanning the three moorings was first filled uniformly to the surface and bottom boundaries. This uniform extrapolation covered on average 10% of the water column at the surface and 12% of the water depth to the bottom. The depth-averaged normal velocity was then calculated. Those mean velocities were multiplied by the cross-sectional areas defined by midpoints between moorings and the coastal boundary. As currents may decrease over the shallow shoulders of each cross section, an estimate of sensitivity was computed by shifting the coastal boundaries by ± 5% of the transect width. Each of the three resulting transport estimates were summed to form an estimate of total transport. Transports were low-pass filtered using a Godin filter to remove diurnal and semidiurnal tidal signals then resampled at 6-h intervals.

2.3. Winds

Winds were obtained from the National Data Buoy Center (NDBC) at two sites. The Cape Spencer (CSPA2) weather station is located at the mouth of Cross Sound, Alaska (58.20°N, 136.64°W). Fairweather Ground (46083) is 105 nautical miles west of Juneau, Alaska (58.27°N, 138.01°W). Additional stations located within the study region at Elfin Cove (ELFA2), George Island (GEXA2), Gustavus Dock (GUXA2), and Bartlett Cove (BLAT2) are not included because their protected locations lead to light and variable wind patterns. Hourly data were obtained from the NDBC web page http://www.ndbc.noaa.gov. Hourly 10 m wind data at the nearest grid point of the ERA5 reanalysis (Hersbach et al., 2018) to NDBC station 46083 was used to compare summer 2010 conditions to reanalysis from 1984 to 2021. Along-shelf and across-shelf components of the wind field from ERA5 and NDBC 46083 were calculated by rotating wind vectors by 324°, the approximate coastline orientation.

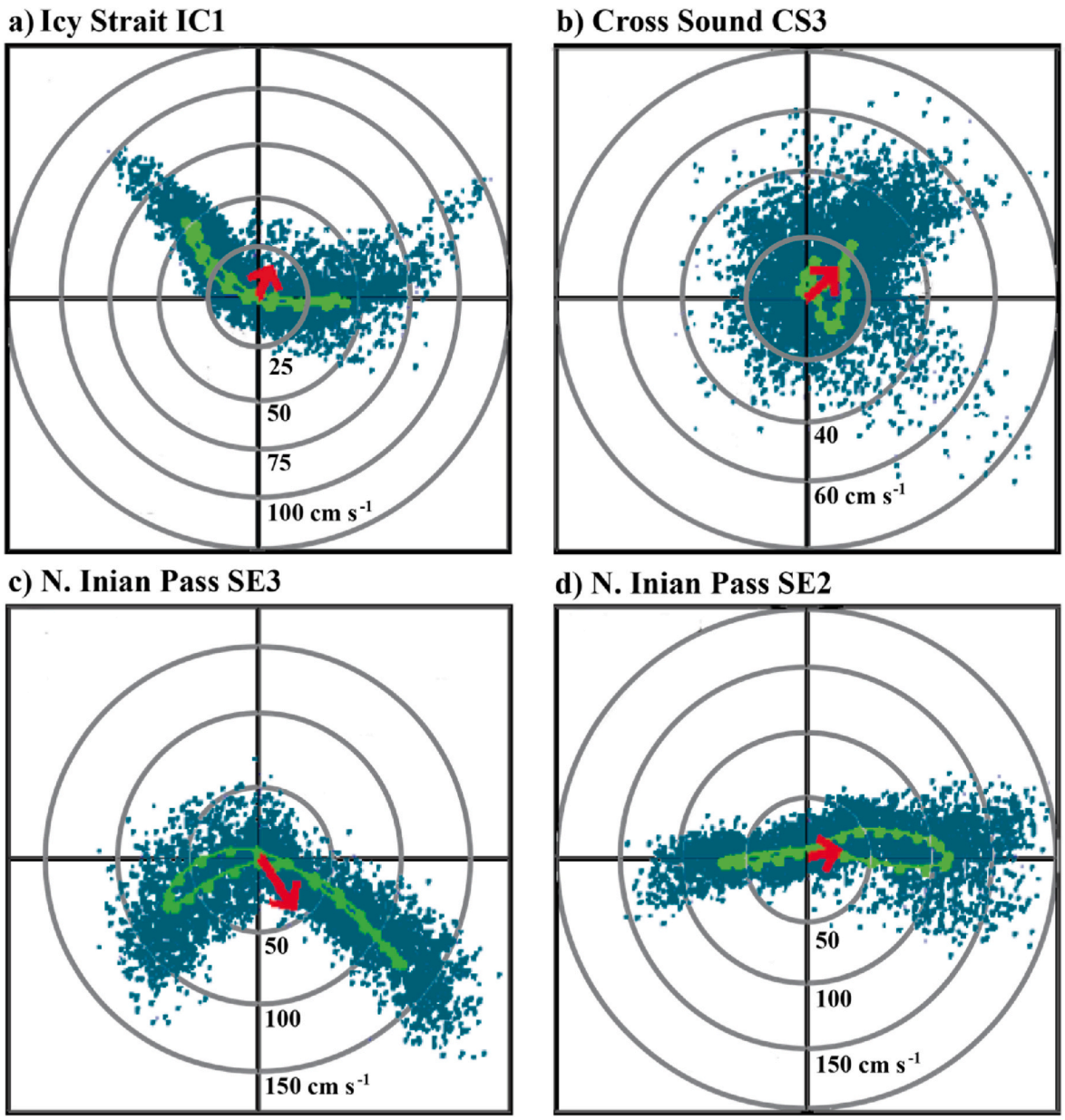

Fig. 2. Scatter plots of near bottom currents for four mooring stations with currents that exhibited a pronounced bend or asymmetry during the tidal cycle. The red arrows are the net velocity and the light green indicates the tidal fit. (For interpretation of the references to color in this figure legend, the reader is referred to the Web version of this article.)

2.4. Bathymetry

Downloading, formatting, proofing, editing, and converting depth soundings into a continuous depth surface followed processes described in Zimmermann and Benson (2013). Soundings from National Ocean Service hydrographic charting surveys within Cross Sound, Icy Strait, Glacier Bay, and some of the surroundings areas were downloaded from the National Geophysical Data Center (http://www.ngdc.noaa.gov/) and plotted in ArcMap (v. 10, ESRI) for examination. The depth soundings from these surveys were collected by lead line, fathometers, or single beam echosounders. Data for most surveys are available as text files that were digitized from the smooth sheets and posted online. In general, the surveys were collected in regional horizontal datums prior to the mid-1940s, in North American Datum of 1927 (NAD27) up to about 1990, and then in North American Datum of 1983 (NAD83). We checked older data sets for correct horizontal datum and shifted them to NAD83, if needed. Typical digitization errors such as incorrect or misplaced soundings were corrected, while missing soundings were digitized from the smooth sheets. The corrected soundings were converted into a Triangulated Irregular Network (TIN) depth surface and the TIN's edges were trimmed to fit within the project area. The TIN was converted into a 100 m horizontal resolution bathymetry raster, and depth contours at 50 m intervals were derived from the raster.

2.5. Satellite images

MODIS true-color images are composites of three wavelengths of MODIS ocean color data: a red band centered at 645 nm; a green band centered at 555 nm; and a blue band centered at 469 nm. The images were created by obtaining the Level-0 MODIS Aqua files from NASA's Ocean Color browser at Goddard Space Flight Center (http://oceancolor.gsfc.nasa.gov). These images were then processed with SeaDAS, a NASA software package available at http://seadas.gsfc.nasa.gov.

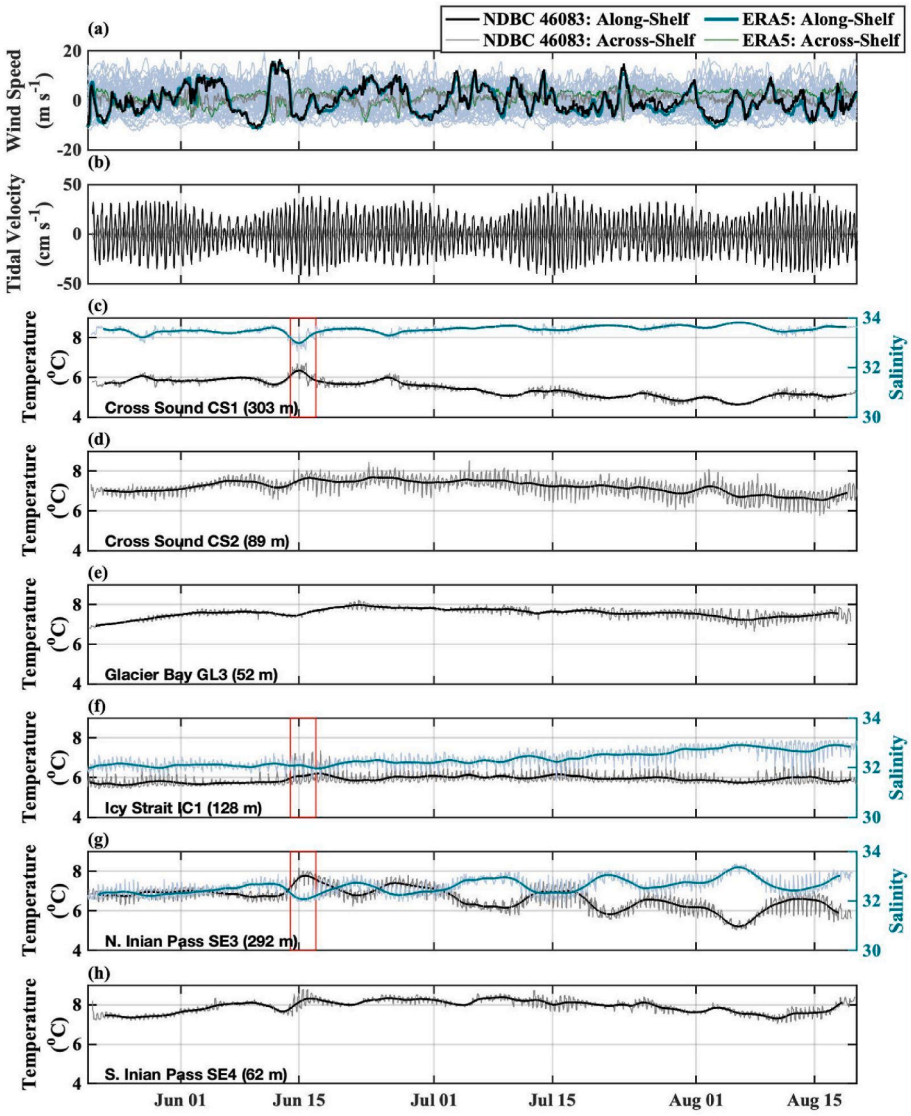

Fig. 3. (A) Along-shelf and across-shelf winds over the shelf from NDBC station 46083 (black and gray lines) and ERA5 reanalysis (green lines) from mid-May to mid-August 2010. Light blue traces show historical winds over the same seasonal time period from 1984 to 2021. (b) Tidal velocities from a harmonic tidal fit to currents at CS1. (c–h) Near-bottom temperature from hourly (thin gray lines) and low-pass filtered (black) data. (c, f, g) At moorings with salinity, hourly (thin green lines) and low-pass filtered (thick green lines) salinity data. Red boxes highlight a 3-day period following strong along-shelf winds. Note that not all stations are shown, as water properties between CS1 and CS3, GL1-3, and between SE2 and SE3 were well correlated. (For interpretation of the references to color in this figure legend, the reader is referred to the Web version of this article.)

2.6. Satellite-tracked drifters

Position data from three satellite-tracked ARGOS drifters, drogued at 40 m with "holey sock" drogues, were examined to estimate spatial flow patterns throughout Cross Sound. One drifter was deployed in May 2011, and two in May 2013 by the EcoFOCI program. Combined, these drifters were tracked for 80 days in Cross Sound. ARGOS position fixes can have errors of 100–300 m (Bograd et al., 1999).

3. Results

3.1. Tidal variability

A harmonic tidal fit was not significant at all sites due to the complexity of the currents (Fig. 2). To obtain the tidal signal at select sites (CS1, GL3, SE4), the near-surface current data were decomposed by least squares harmonic analysis into 27 individual harmonic constituents consisting of phase and amplitude along a major and minor axis of flow using the T-Tide analysis package (Pawlowicz et al., 2002). Tidal energy accounted for 96, 92, and 98% of the kinetic energy throughout the water column at CS1, GL3, and at SE4, respectively. Tidal velocities are predominantly a mixed semi-diurnal pattern at the M_2 frequency with fortnightly variability (e.g., Fig. 3b).

Comparing sites CS1 and GL3, which had statistically significant tidal fits, the peak correlation in surface tidal currents was at 0-lag; the tide flows in phase throughout Cross Sound. The high speeds of the tidally forced currents at three moorings (IC1, CS3, and SE3) ebbed and flooded along different principal axes, steered by channel curvature (Fig. 2a–c). Taking a simple average of currents with such a bend results in an average vector in the direction of the angle created by the ebb and flood currents. Because of this, mean current speed and direction were calculated for ebb and flood periods separately (Fig. 1 and Table 1).

Near-bottom temperature and salinity also varied at tidal frequencies, although the magnitude of the semidiurnal and fortnightly tidal variability was not the same at every location (Figs. 3 and 4). Temperature and salinity were decomposed by least squares harmonic

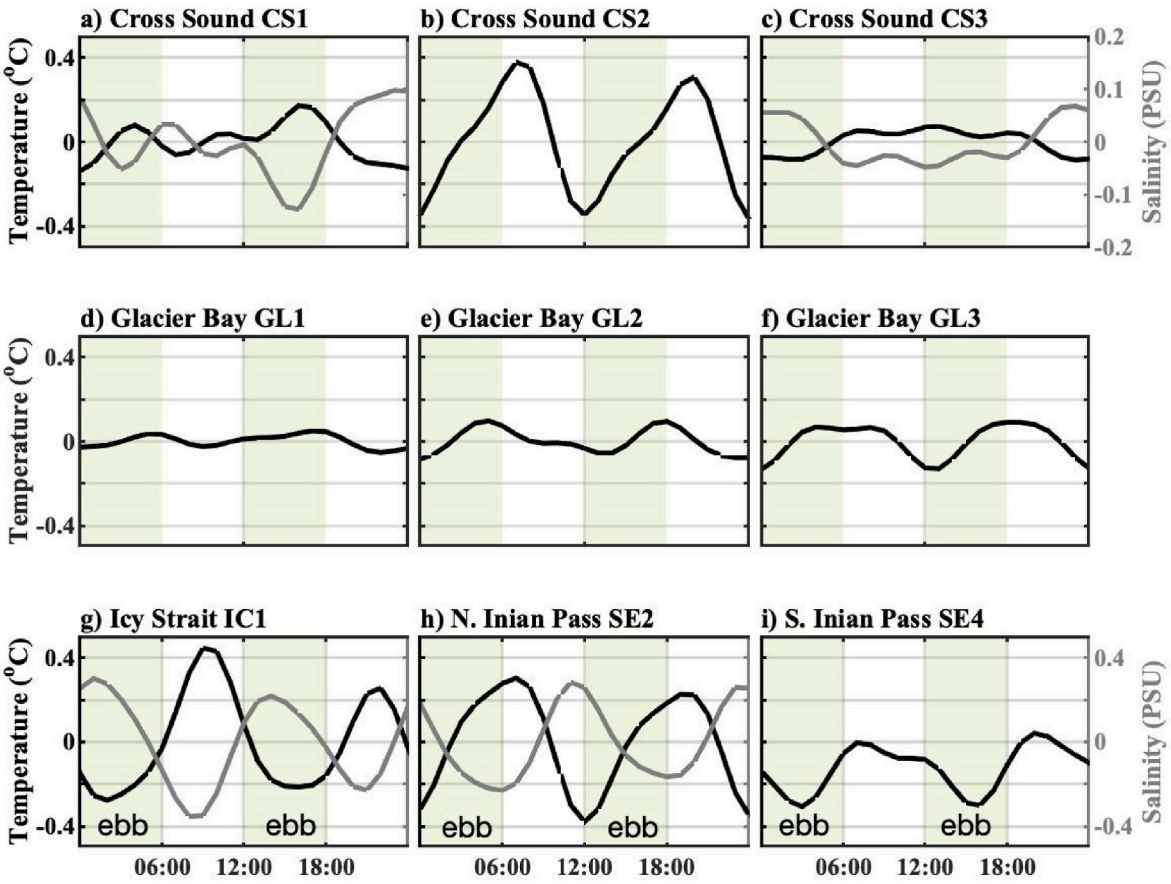

Fig. 4. A sample of a single tidal cycle of temperature (black) and salinity (gray) variability from each station using a tidal harmonic fit. Green shaded periods indicate ebb tides. Temperature (black) and salinity (gray) time series were fit to tidal harmonics to estimate the variance. (For interpretation of the references to color in this figure legend, the reader is referred to the Web version of this article.)

analysis to estimate the tidal variability while low (subtidal) and higher frequency variability were separated using a low-pass Godin filter (Thomson and Emery, 2014).

3.2. Observations by region

3.2.1. The entrance to Cross Sound

The entrance to Cross Sound is a 13 km opening where the nutrient rich, low salinity water of Cross Sound exchanges with the more saline Gulf of Alaska (Stabeno et al., 2016b). The combination of the complex bathymetry, the length of the opening, which is approximately the Rossby radius, and a large tidal range (>5 m) causes complex behavior at the three stations transecting the opening. Mean transport is laterally sheared, with net flow from the Gulf of Alaska into Cross Sound to the south and out of Cross Sound through the northern portion of the opening (Fig. 5a).

The northern side of the mouth (Fig. 1), the location of CS2, is relatively shallow (~95 m) and the speed was the fastest of the three stations (CS1, CS2, CS3; Table 1). At CS2, mean outflow exceeds inflow. The mean ebb current exceeded flood at all depths, but decreased with depth from >65 cm s^{-1} near the surface to ~40 cm s^{-1} near the bottom. While flood speeds were more consistent through the water column, the principle axis of flood currents ranged from nearly eastward at the surface to a more northeastward orientation of ~40° T near the seafloor.

Station CS1, the center mooring, exhibits classical estuarine flow with outflow near the surface and inflow near the bottom with a mid-depth null point (Fig. 6d–f). This transition depth shoals through the spring, but remains relatively constant from June into the fall (Stabeno et al., 2016b). The bathymetry to the north diverts the flow at depth north and south but upper layers move northeast to southwest. The currents exhibit a strong fortnightly signal, particularly in the bottom layers (Fig. 6f).

The southern station, CS3, exhibited a rotary tidal current (Fig. 2b). At CS3, there was tidally averaged inflow for most of the deployment period (Fig. 5a), with a maximum speed of 127 cm s^{-1} during flood (Table 1).

A fortnightly signal is also apparent in the near-bottom temperature and salinity at the deeper sites CS1 and CS3 (e.g., Fig. 3c; note that CS3 is not shown because water properties were well correlated between CS1 and CS3) driven by tidal variability and mixing (Stabeno et al., 2016b). Spring tides were associated with warmer and fresher bottom water. The mean tidal range in temperature and salinity also varied between the stronger and weaker of the mixed semidiurnal tidal periods (Fig. 4a–c). While low-passed filtered temperatures were strongly correlated at the deeper locations CS1 and CS3, the same fortnightly variability did not dominate at the shallower Cross Sound site CS2, where temperature variability was dominated by the semidiurnal tidal oscillation (Fig. 3d).

3.2.2. Flow around the Inian Islands

Three moorings were deployed around the Inian Islands (Fig. 1). SE4 was deployed in a constriction south of the largest island in 67 m of water. The bathymetry in the region is complex, shoaling considerably compared to north and west of the islands, creating large variability in velocities over relatively short horizontal distances. Because of the great need for navigational information, two stations (SE2 and SE3) were deployed north of the Inian Islands to understand the flows through this narrow, treacherous pass. This 3-km wide constriction between Inian Island and Point Wimbeldon is the main passageway between east and

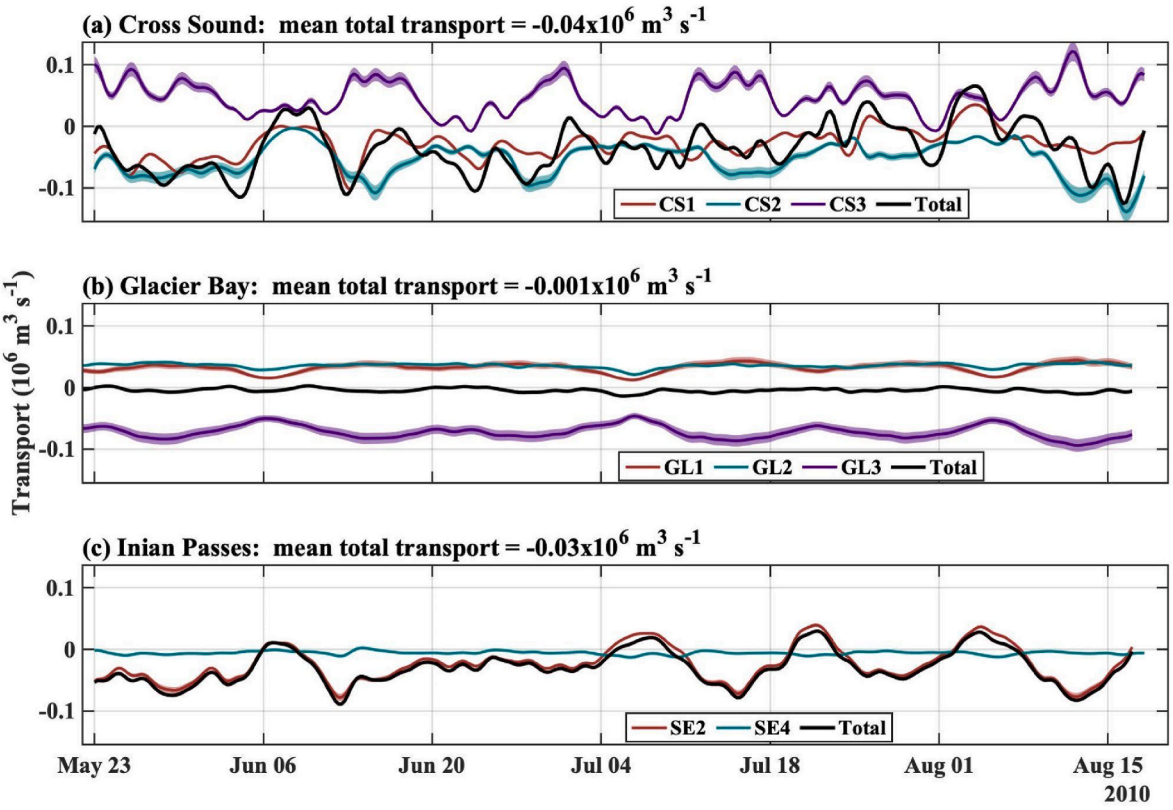

Fig. 5. Transports measured at (a) the mouth of Cross Sound, (b) Glacier Bay, and (c) Inian Pass. Positive transports are in the upstream direction, approximately eastward at Cross Sound and Inian Pass and northward at Glacier Bay. Light shading around transports indicates the sensitivity to the definition of the coast. The time-mean cross-sectionally averaged transport is reported for each cross section.

west Cross Sound resulting in large volumes of tidal flow. The initial project design was to orient stations SE2 and SE3 to span a single section across the channel, but the strong currents presented challenges. The two ADCPs in this pass were deployed 900 m apart along the 58.28° parallel. The orientation of these two moorings along-channel from each other allows for an examination of the influence of bottom bathymetry on these flows. The placement of SE3 was closer to a seamount than SE2. Interestingly, even a separation distance of less than a kilometer had a great effect on the flow pattern.

Station SE2 and SE3 recorded maximum speeds of 187 and 258 cm s^{-1}, respectively. Fig. 2c shows the current at station SE3 throughout the deployment. Note the inflection that exists between the near-bottom flood and ebb currents. This inflection persists throughout the water column with a depth-average flood direction of ~93° T, opposed to the ebb direction at ~237° T (Table 1). The subsurface seamount directs flood water to approach SE3 from the northwest instead of the west as expected. The ebb currents from the northwest flow past SE3 and are diverted to the right. In contrast, station SE2 exhibits a rectilinear primarily east-west flow (Fig. 2d). Not surprisingly, the near bottom currents at SE2 and SE3 are highly correlated (complex correlation of R^2 = 0.84), with a rotation angle of 20°. This directional offset is not likely a compass error because the periodic rotation of the current direction at SE3 corresponds with the tidal period. At both sites, the time-averaged flow shows a similar estuarine exchange pattern. Deep water has a net eastward flow into the Sound and surface flow has a net westward flow towards the mouth of Cross Sound (Fig. 6a–c).

Although shallower, SE4 had similar mean ebb and flood currents as stations SE2 and SE3 to the north (Table 1). Maximum ebb currents of 74 cm s^{-1} toward 241° T were slightly faster than the maximum flood currents of 52 cm s^{-1} (Table 1). The semidiurnal tides dominate the flow through South Inian pass with M_2 constituent contributing close to 90% of the total energy of the flow.

As expected, the near bottom temperature and salinity were strongly correlated between sites SE2 and SE3 with R^2 = 0.94 and R^2 = 0.84, respectively. The magnitude of semidiurnal variability is similar to that of the fortnightly in both temperature and salinity (Fig. 3g). Bottom waters became warmer and fresher during ebb tide (Fig. 4h) suggesting advection from the warmer waters in Glacier Bay (Table 2). SE2 and SE3 also recorded warmer and fresher bottom waters during spring tides (Fig. 3g), suggesting local mixing of surface waters associated with stronger tidal friction. To the south of the Inian Islands, SE4 had the warmest mean temperatures of all the moorings deployed, even compared to sites CS2 and GL1-3 at similar depths (Table 2). Near-bottom temperatures at SE4 warmed during peak ebb (Fig. 4i), possibly due to increased local mixing during the strongest phase of the tidal currents.

3.2.3. *The entrance of Glacier Bay*

Glacier Bay opens onto the north side of Cross Sound with a mouth that is 6.5 km wide. Three moorings were placed across the mouth to determine the flow patterns between Glacier Bay and Cross Sound. The mean circulation had well-correlated inflow at the two eastern moorings (GL1 and GL2) with strong outflow at the western mooring (GL3; Fig. 1). Although there is not a full reversal in the currents through the water column, there is vertical shear with stronger outflow near the surface than at the bottom (Fig. 7). The vertical shear is driven by the outflow of relatively fresh surface water from inside of Glacier Bay. Both horizontal (east to west) and vertical shear are expected due to the width (approximately the Rossby radius) of the opening. Hill et al. (2009) determined there was a net outflow from Glacier Bay of <0.01 Sv caused by runoff. We also estimated a small mean transport at the mouth, with inflow at the two eastern moorings approximately balancing the outflow in the western side of the mouth (Fig. 5b).

The temperatures near the seafloor were similar across stations GL1-

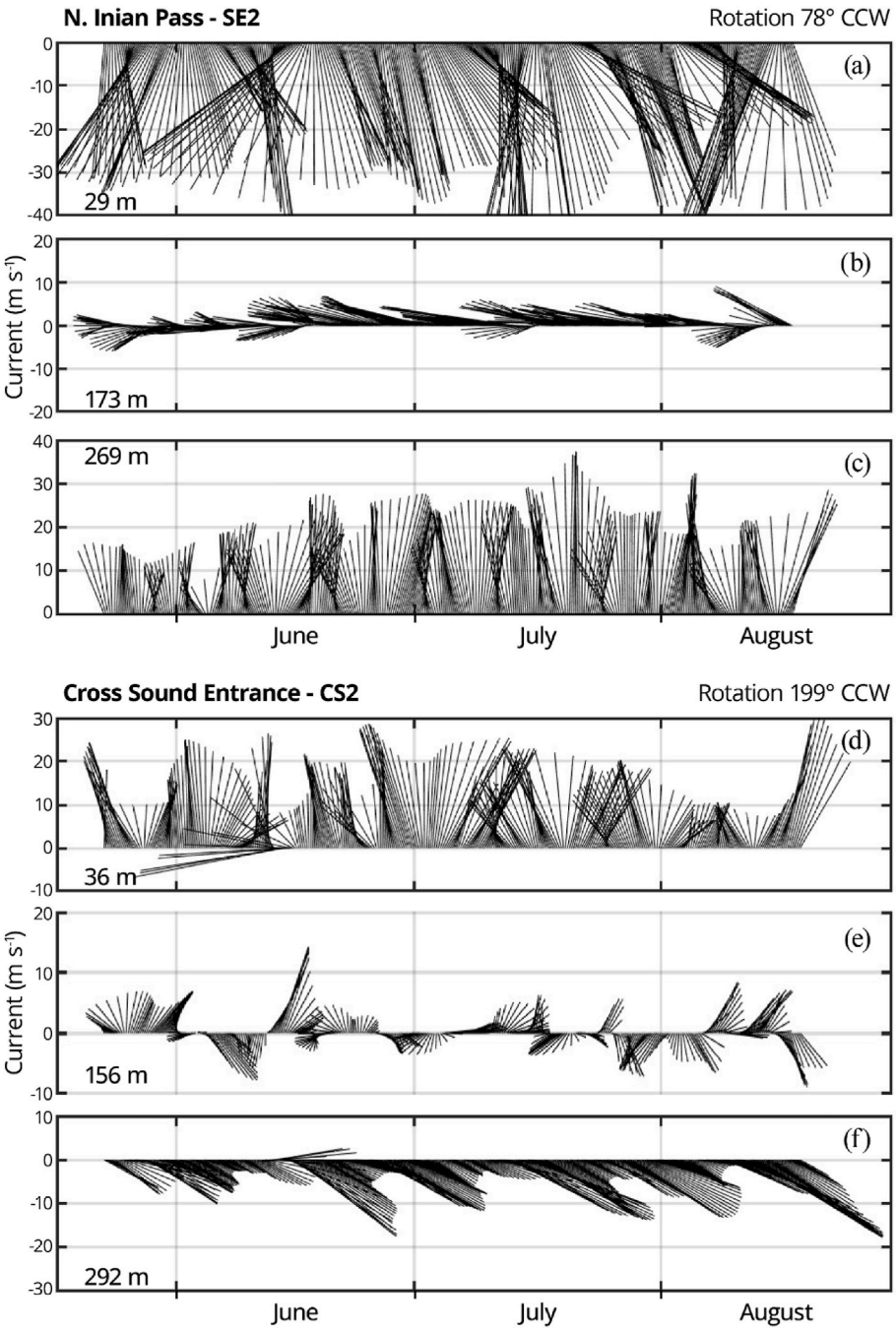

Fig. 6. Low-pass filtered velocities at North Inian Strait (top panels) and Cross Sound Entrance (bottom panels) from mid-May to mid-August 2010. The depths are noted on each panel. The angle of rotation is indicated for each mooring.

3 (Table 2). Temperature peaked in late June, and decreased throughout July. Although a fortnightly signal persists in the low-pass filtered transports at all stations, fortnightly temperature variability was smaller than monthly and semidiurnal patterns. The semidiurnal tidal variability was small early in the summer, but reached ~1 °C in August; the tidal temperature range tended to be greatest during neap tides (Fig. 3e). These patterns were qualitatively similar across all three sites GL1-3, although the magnitude of tidal variability increased slightly from east-to-west (Fig. 4d–f; Table 2). Greater semidiurnal temperature variability in late summer and during neap tides, when the water column would be more strongly stratified, indicate local mixing of vertical gradients that are advected past these moorings. On average, bottom temperatures increased during ebb and decreased during the flood, particularly in late summer (Fig. 4d–f), suggesting a horizontal gradient with warmer bottom temperatures inside of Glacier Bay than outside in Cross Sound or Icy Strait.

3.2.4. *Icy Strait*

Icy Strait is a deep (>100 m) channel that ranges in width from ~9 km in the south to 18 km in the north. Maximum speeds at IC1 were 138 cm s^{-1} (Table 1). The axis of flow differed by ~50° between flood (91° ± 5°) and ebb (320° ± 4°) flow (Fig. 2a). The vertical structure of the current speed had three layers. At the top ADCP bin and below 90 m depth, the mean current was in the ebb-direction, but at mid-depths the mean current was upstream in the flood-direction. This section is not shown because Icy Straight likely exhibits across-channel structure as at

Table 2
List of the sensor depth at each mooring and the record-mean and linear trends of temperature and salinity. The standard deviation from the mean temperature is calculated from the high-pass filtered time series to provide an estimate of tidal variability. The trend is calculated from a linear regression using the full time series and reported in the estimated linear change in temperature or salinity over the 90-day record length (mid-spring to mid-summer).

Mooring (inst. depth)	Mean Temperature (°C) Salinity	Change per 90 days Temperature (°C) Salinity
CS1 (309 m)	5.4 ± 0.1	−1.21 ± 0.03
	33.5 ± 0.1	0.27 ± 0.02
CS2 (89 m)	7.2 ± 0.3	−0.51 ± 0.06
	–	–
CS3 (311 m)	5.3 ± 0.1	−1.22 ± 0.03
	33.6 ± 0.1	0.28 ± 0.02
GL1 (57 m)	7.5 ± 0.1	−0.06 ± 0.04
	–	–
GL2 (63 m)	7.7 ± 0.1	−0.13 ± 0.04
	–	–
GL3 (52 m)	7.6 ± 0.2	0.02 ± 0.04
	–	–
IC1 (128 m)	5.9 ± 0.2	0.17 ± 0.04
	32.4 ± 0.2	0.90 ± 0.03
SE2 (287 m)	6.7 ± 0.2	−1.07 ± 0.06
	32.6 ± 0.2	0.55 ± 0.05
SE3 (292 m)	6.6 ± 0.2	−1.16 ± 0.07
	32.6 ± 0.2	0.56 ± 0.04
SE4 (62 m)	7.9 ± 0.1	−0.01 ± 0.05
	–	–

the mouths of Cross Sound and Glacier Bay, and a single central mooring may not represent the full channel variability.

Icy Strait is shallower than the adjacent channels of North Inian Pass and Chatham Strait, connecting Cross Sound to Southeast Alaska's inside passages. This relatively shallow area may act as a local mixing zone as tides advect water over the sill. There is large tidal variability in the near-bottom temperature and salinity over both the semi-diurnal and spring-neap time scales (Fig. 3f). During spring tides, temperatures can vary by > 1 °C and salinities by > 1 each tidal cycle. This spring tidal range appeared to increase throughout the summer, likely because of surface warming during summer that is mixed downward by the tidal currents. There is also an asymmetry in the water properties between flood and ebb tide (Fig. 4g), likely due to the different source waters advected past the site during ebb (from Icy Strait) and flood (from Cross Sound).

4. Discussion

This array of 10 moorings deployed in the summer of 2010 provides a baseline for studying the complex exchange, tidal currents, and bottom water properties throughout Cross Sound to Icy Strait. While this study yields information about the dynamics in four regions of Cross Sound, a complete picture of the complex flows and water mass budgets was not possible due to logistical limitations. For example, only near-bottom water properties were measured because of the strong currents, regular ship traffic, and fishing activity in the area. Also, a complete picture of the complex flow in Icy Strait cannot be derived from the lone mooring that was deployed.

4.1. Mean circulation throughout Cross Sound

An estimate of the mean circulation throughout Cross Sound was mapped using current observations from the moorings, coupled with data from satellite-tracked drifters from the summers of 2011 and 2013 (Fig. 8). Mean near-surface currents (Fig. 8a) were derived from mooring time series (solid arrows) and extrapolated using satellite tracked drifter trajectories (drogue depth 40 m) as a guide (dashed arrows). Drifter tracks provide a snapshot of circulation pathways and tidal excursion lengths. One drifter (Fig. 8a, red line) was inside of Cross Sound for ~11 days and spent ~8 days east of the Inian Passes. This drifter circled Lemesurier Island and entered Glacier Bay twice during two tidal excursions. Two other drifters (not shown) remained west of the Inian Passes, primarily along the coastal boundaries near the entrance to Cross Sound occasionally being advected across the channel. The tidal excursions observed from these drifter tracks vary over time due to the spring-neap cycle and mixed tides in this region, but several representative examples are illustrated in Fig. 8c. The mean near-bottom circulation (Fig. 8b) was mapped using the mooring time series (solid arrows) and extrapolated following channels in the bathymetry (dashed arrows). In the shallow region between Lemesurier and Pleasant Islands and extending into Glacier Bay, the extrapolated bottom currents were also informed using the drifter trajectories. Large tidal excursions through this shallow region suggest a high degree of connectivity throughout this whole region.

4.2. Mean spatial patterns from 2010

This array of moorings provides insight into the variability of temperature and salinity of near-bottom waters throughout the Cross Sound region. Although the spatial distribution of stations is coarse, there is an along-channel gradient in water properties with cooler and saltier water at the mouth of Cross Sound, relatively warmer water around Inian Island, and cooler and fresher water around Icy Strait (Table 2). CS1 and CS3 have cooler mean temperatures than SE2-3 in North Inian Pass by $>$ 1 °C (Table 2). Amongst shallower stations, mean temperatures were also cooler near the ocean entrance to Cross Sound at CS2 than at the Glacier Bay entrance GL1-3, and were warmest at SE4 in South Inian Pass. Relatively warmer bottom waters within Cross Sound is consistent with previous observations of cooler surface temperatures within Cross Sound than over the shelf due to local mixing of cold waters from depth (Etherington et al., 2007). Furthest from the mouth, mooring IC1 at the entrance to Icy Strait measured a cooler mean temperature (5.9 °C) than any of the shallow stations and cooler, even, than the deeper stations in North Inian Pass (Table 2). Strong surface warming and summer stratification in Icy Strait may isolate cooler water at depth that is advected over this sill by the tidal currents (Park et al., 2004).

The salinity was measured only on the deeper moorings so were limited to stations CS1, CS3, IC1, and SE2-3. Mean salinities at SE2 and SE3 in North Inian Pass were fresher by > 1 than at stations CS1 and CS3 located closer to the ocean entrance to Cross Sound. The freshest mean salinity was from station IC1 at 128 m depth. At the mouth (CS1) the tidal range of salinity remained relatively constant while temperatures cooled throughout the summer as stratification reduced mixing between the surface waters and depth (Fig. 3c). During 14–17 June 2010 the bottom waters throughout Cross Sound were anomalously fresh and warm (Fig. 9). This event was associated with the warmest and freshest near-bottom waters observed in North Inian Pass (SE3), but the anomalies during this time period at SE3 were small relative to the tidal range (Fig. 3g). The water mass properties at SE3 are more similar to oceanic conditions represented at CS1 at the end of each flood during neap tides (Figs. 3g and 4h). The Icy Strait mooring IC1 is shallower than CS1 and SE3, complicating the comparison of water properties between these three regions of Cross Sound. At IC1 a bulb in the temperature-salinity diagram indicates the convergence of at least three water masses at this site (Fig. 9c). Here, warming temperatures through July are consistent with the seasonal trend in sea surface temperature (Park et al., 2004). Cooler and saltier conditions in August indicate advection of deeper water over the sill at Icy Strait.

Local tidal mixing from bottom friction appears to be the primary driver of the near-bottom temperature and salinity variability. In the deep channels throughout Cross Sound, bottom water properties are fairly consistent in the summer with variability primarily driven by the tides at semidiurnal and fortnightly frequencies (Fig. 3c–g). At deeper sites in this study, fortnightly variability is greatest, while at shallower

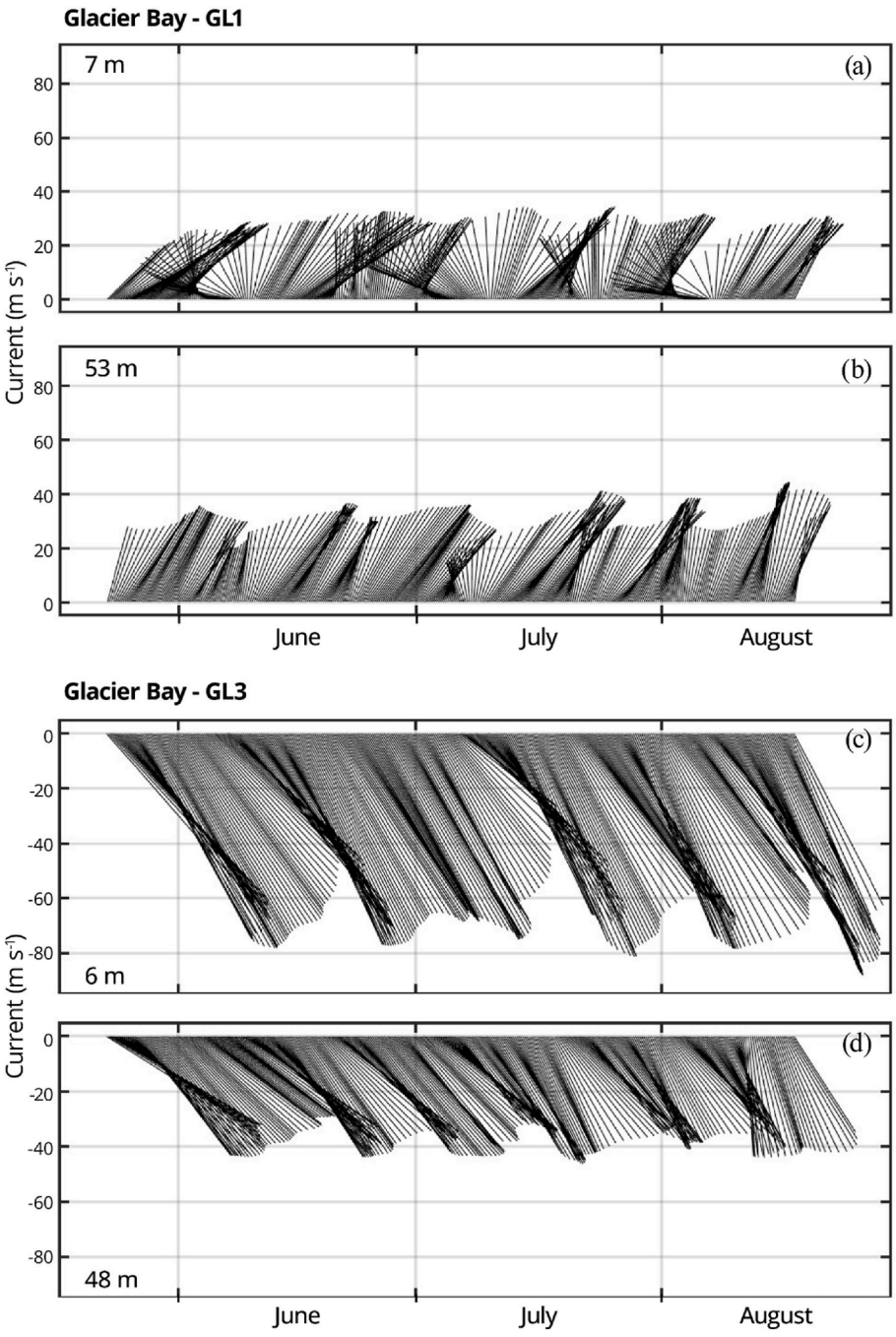

Fig. 7. Similar to Fig. 6, except from Glacier Bay GL1 (top panels) and GL3 (bottom panels).

sites variability is greatest on semidiurnal timescales. Over the period from 12–15 June 2010 bottom temperatures at CS1 near the mouth of Cross Sound increased rapidly by > 1 °C over the 3-day period, coinciding with spring tides and anomalously strong summer wind speeds that likely increased local water column mixing over this period (Fig. 3a and b). Comparing temperature variations at CS1 from June to August in 2011 and 2013 (Stabeno et al., 2016b), rapid changes of >1 °C may not be a common occurrence for bottom waters in Cross Sound, but climatological changes such as increased wind events or weakened stratification due to a seasonal shift in the peak discharge from summer to fall could increase the synoptic temperature variability at depth. Although coastal freshwater discharge increased throughout the summer, bottom salinities at stations in 2010 either increased or remained constant throughout the summer deployment period studied here (Table 2). The slight mean salinity increase of about 0.5–1 over 90 days through North Inian Pass and Icy Strait suggest the development of stratification and reduced vertical mixing.

4.3. Seasonal and interannual variability at the Cross Sound entrance

Observations from fall through spring and in other years are compared to contextualize this study that focuses on measurement during the summertime period from 20 May through August 20, 2010. These longer-term observations show that over the shelf offshore of Cross Sound, summer is the season with the least variability in bottom temperature and salinity, characterized by relatively cool and salty water (e.g., Stabeno et al., 2016b). Measurements at CS1-3 in 2011 and 2013 published by Stabeno et al. (2016b) were centered around the

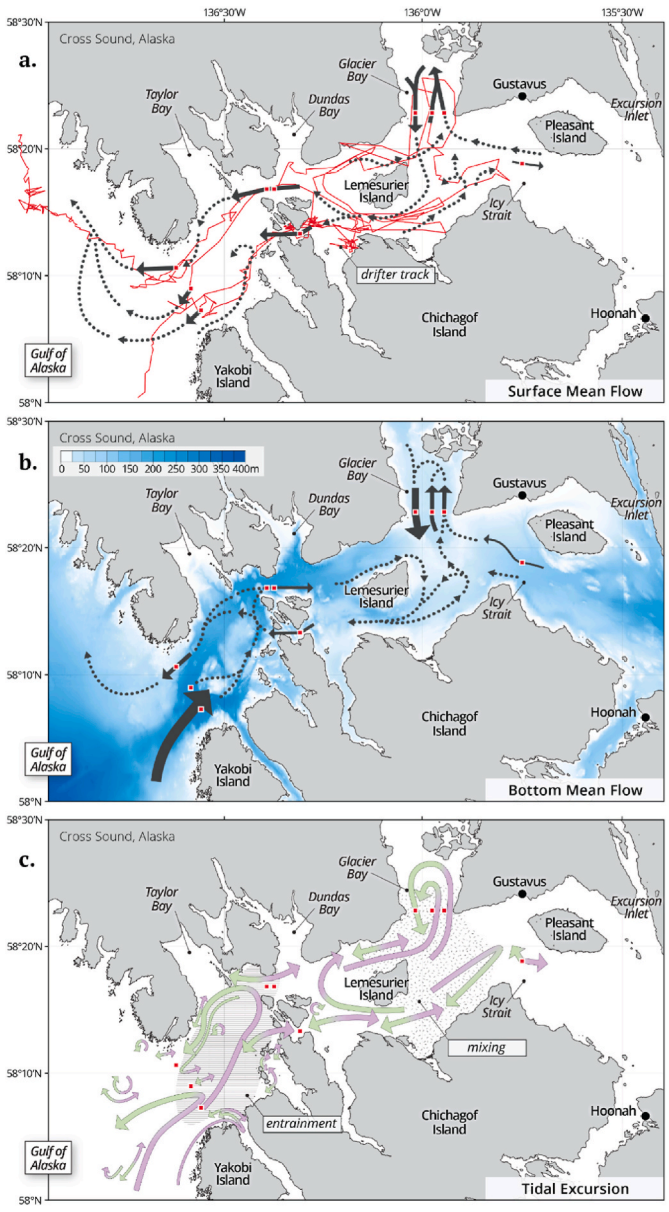

Fig. 8. Summary diagrams of approximate mean (a) near-surface currents with satellite tracted drifter trajectory (red), (b) near-bottom currents, and (c) tidal excursion distances throughout Cross Sound in summer. Dashed lines are based on drifter observations and bathymetry. The red trace in (a) maps locations of a satellite-tracked drifter from 16 April to October 19, 2013. In (c) shading indicates regions where surface and bottom currents are similar due to strong mixing; hatching indicates a region where shoaling likely contributes to entrainment of bottom waters into the surface layer. Tidal excursions (flood direction in purple, ebb direction in green) are sampled from drifter tracks, but vary over time due to the spring-neap cycle and mixed tides in this region; distances are approximate. Credit: Sarah Battle, NOAA/PMEL. (For interpretation of the references to color in this figure legend, the reader is referred to the Web version of this article.)

summer season, but began as early as 1 February and data collection lasted as late into the fall as 10 November. For seasonal comparison, fall and winter data from 2005 to 2007 at CS1 is also considered (Fig. 10). The greatest synoptic variability in bottom water properties over the shelf and across the mouth of Cross Sound is in the spring and fall (Stabeno et al., 2016b). From fall and winter measurements, the fortnightly tidal variability is the dominant subseasonal signal in the bottom temperature and salinity at CS1 (Fig. 10). From May to October, increases in bottom temperature correspond with dips in salinity at CS1 (Fig. 3c and 10), but from around December 2006 through February 2007 there was less temperature variation than observed salinity variability (Fig. 10b). In early spring 2007, temperature increases correspond with increasing salinity–the opposite pattern as from summer and fall observations. In spring the surface waters are likely cooler than the bottom and the water column is stratified by salinity (e.g. Stabeno et al., 2016b).

4.4. Ecological implications

A true-color satellite image captured a phytoplankton bloom throughout Cross Sound during clear skies in mid-September 2010 (Fig. 11). This feature was observed following a spring tide and a 5 day period of relatively calm winds. The feature covers Cross Sound and extends onto the shelf, to the north where there is outflow from Cross Sound. The bloom is not evident over the southern portion of the mouth where the mean transport is into Cross Sound (Fig. 5a). We hypothesize that strong vertical mixing associated with the spring tide delivered a pulse of nutrients to the euphotic zone to support the onset of a phytoplankton bloom within Cross Sound, and nitrate was also exported from Cross Sound to the northwest to support additional primary productivity over the shelf (Stabeno et al., 2016b).

This annual cycle of across-shelf exchange, where dense nutrient-rich bottom waters are upwelled over the shelf during summer periods when downwelling winds relax and is vertically mixed into the euphotic zone by regional coastal physical processes drives the high primary productivity along the Gulf of Alaska shelf (Childers et al., 2005). The exchange of shelf water through Cross Sound is funneled by the bathymetry of the Yakisoba Sea Valley and enhanced by the estuarine circulation and entrainment (e.g., Burchard et al., 2018). The exchange generates a regional hotspot for chlorophyll blooms (Waite and Mueter, 2013), export of riverine iron and silicate into locally formed shelf eddies (Ladd and Cheng, 2016), and for accumulation of larvae spawned offshore that rely on physical mechanisms to access suitable habitats over the shelf and inshore waters (Goldstein et al., 2020). Within Cross Sound, the mixing of oceanic waters with riverine discharge and glacial melt over the shallow sill at Icy Strait supports a highly productive and diverse ecosystem (e.g., Weingartner et al., 2009). The fronts in Icy Strait and Glacier Bay are apparent in satellite chlorophyll images (Fig. 11). There is significant inter-annual variability in the ecosystem response to oceanic conditions from shifts in copepod biomass and size (Park et al., 2004) to impacts on humpback whale reproductive success and survival (Gabriele et al., 2022). A climatological increase in summertime wind events, as the one observed around 12–15 June 2010, or a shift in the buoyant discharge peak from summer into the fall could reduce summertime stratification in Cross Sound. Reduced stratification could enable more vertical mixing of nutrients and increase synoptic variability of bottom temperatures. A later spring freshet can also impact the magnitude and timing of the spring phytoplankton bloom (e.g., Stabeno et al., 2016b).

5. Conclusions

There have been limited observations of the bottom water properties and water column currents in Cross Sound. Currents from 10 locations throughout Cross Sound demonstrate bathymetric steering of tidal currents and tidal mixing throughout the water column. Strong currents at multiple sites have a bend in the tidal flow, with mean flood and ebb currents that are not parallel to each other. At moorings across the mouth of Cross Sound and in North Inian Pass, there is a net exchange flow with currents into Cross Sound near the bottom and outflow in the surface layer. Summer mean water properties had a spatial gradient with cooler and saltier water near the mouth of Cross Sound, cooler and fresher water around Icy Strait, and relatively warmer water around Inian Island. There is a fortnightly signal in the low-pass filtered transport and bottom currents, which corresponds with temperature and

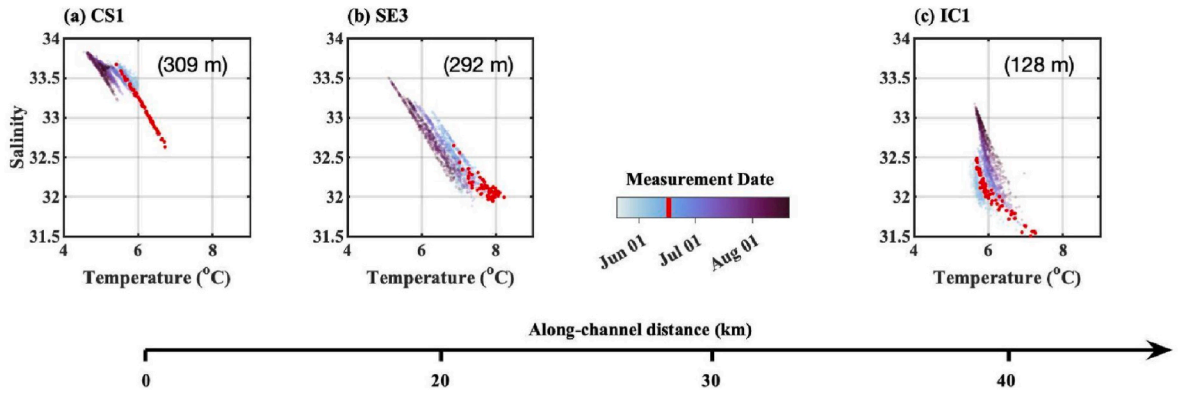

Fig. 9. Comparisons of near-bottom temperature and salinity at (a) CS1 near the mouth of Cross Sound, (b) SE3, and (c) IC1. Points are shaded by the time of the measurement. Red points correspond with the time period highlighted with a red box in Fig. 3. (For interpretation of the references to color in this figure legend, the reader is referred to the Web version of this article.)

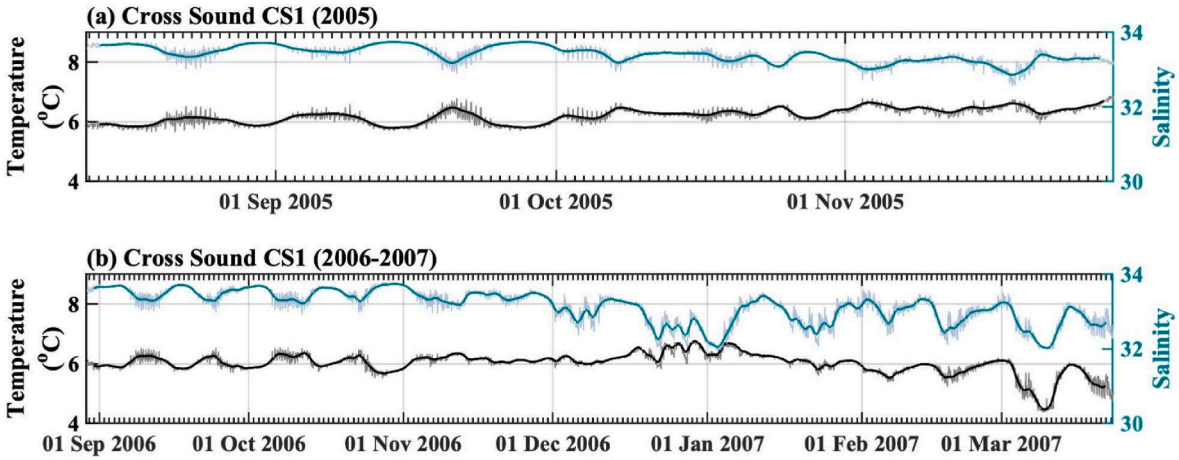

Fig. 10. Similar to Fig. 3c, but showing near-bottom temperature (black) and salinity (green) from CS1 during (a) fall 2005, and (b) fall 2006–spring 2007. (For interpretation of the references to color in this figure legend, the reader is referred to the Web version of this article.)

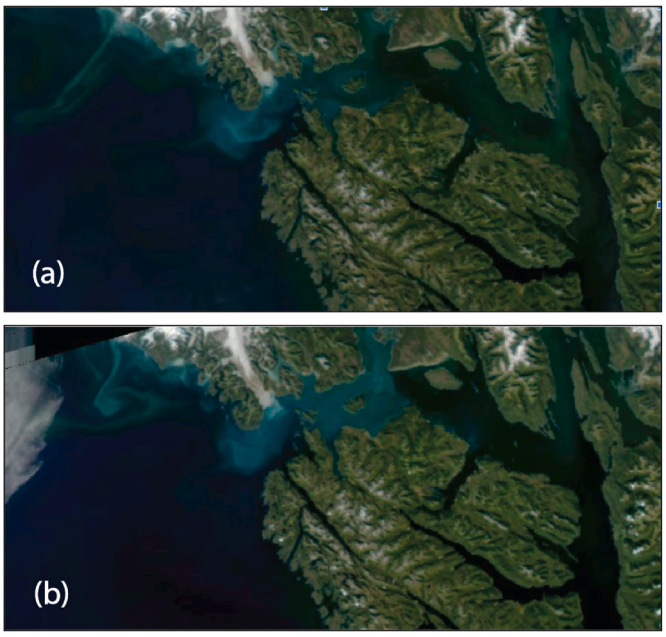

Fig. 11. True color images from (a) September 13, 2010 and (b) September 14, 2010. (For interpretation of the references to color in this figure legend, the reader is referred to the Web version of this article.)

salinity variability. At shallower moorings, temperature and salinity had a greater semidiurnal variance and relatively weaker fortnightly variability. These measurements provide a baseline of the area's tidal energy, circulation, and bottom water properties. Although the dynamics are dominated by the tides, anomalous water properties in mid-June were associated with spring tides and anomalously strong summer wind speeds. Predicted climatological shifts such as decreased freshwater discharge in summer and higher frequencies of strong wind events could lead to decreased stratification and an increased occurrence of deep advection and mixing events in these waterways. Increased mixing could provide a pathway for more nutrient exchange between deep waters and the surface and may lead to more variable bottom temperatures along these benthic habitats in summer.

CRediT authorship contribution statement

Emily Lemagie: Writing – review & editing, Writing – original draft, Visualization, Validation, Supervision, Software, Resources, Project administration, Methodology, Investigation, Funding acquisition, Formal analysis. **Christopher Paternostro:** Writing – review & editing, Writing – original draft, Visualization, Validation, Supervision, Software, Resources, Project administration, Methodology, Investigation, Funding acquisition, Formal analysis, Data curation, Conceptualization. **Phyllis J. Stabeno:** Writing – review & editing, Writing – original draft, Visualization, Validation, Supervision, Software, Resources, Project administration, Methodology, Investigation, Funding acquisition,

Formal analysis, Data curation, Conceptualization. **Mark Zimmermann:** Writing – review & editing, Writing – original draft, Visualization, Validation, Supervision, Software, Resources, Project administration, Methodology, Investigation, Funding acquisition, Formal analysis, Data curation, Conceptualization.

Declaration of competing interest

The authors declare that they have no known competing financial interests or personal relationships that could have appeared to influence the work reported in this paper.

Acknowledgements

The authors would like to acknowledge the field team for their work with deploying the moorings, and David Kachel for processing the data. This work was funded by NOAA. This is NOAA PMEL contribution 5555 and Ecosystems Fisheries Oceanography Coordinated Investigations (EcoFOCI) contribution 1043. CO-OPS data used in this study are available from https://tidesandcurrents.noaa.gov/cdata/ (keyword search SEA10); EcoFOCI Cross Sound data are available from https://doi.org/10.25921/4qne-j435 (mooring CS1, 2005 and 2006), https://doi.org/10.25921/8fmc-1q11 (mooring CS1, 2011), https://doi.org/10.25921/98zn-f138 (mooring CS1, 2013), and https://doi.org/10.25921/zc88-yk50 (all 10 moorings, 2010).

Data availability

Data will be made available on request.

References

Bograd, S.J., Thomson, R.E., Rabinovich, A.B., LeBlond, P.H., 1999. Near-surface circulation of the northeast pacific ocean derived from WOCE-SVP satellite-tracked drifters. Deep sea res. Part II: topical stud. Oceanography 46 (11–12), 2371–2403.

Burchard, H., Bolding, K., Feistel, R., Gräwe, U., Klingbeil, K., MacCready, P., et al., 2018. The knudsen theorem and the total exchange flow analysis framework applied to the baltic sea. Prog. Oceanogr. 165, 268–286. https://doi.org/10.1016/j.pocean.2018.04.004.

Childers, A.R., Whitledge, T.E., Stockwell, D.A., 2005. Seasonal and interannual variability in the distribution of nutrients and chlorophyll a across the Gulf of Alaska shelf: 1998–2000. Deep Sea Res. Part II: topical Stud. Oceanography 52 (1–2), 193–216. https://doi.org/10.1016/j.dsr2.2004.09.018.

Connor, C., Streveler, G., Post, A., Monteith, D., Howell, W., 2009. The neoglacial landscape and human history of Glacier Bay, Glacier Bay National Park and preserve, southeast Alaska, USA. Holocene 19 (3), 381–393. https://doi.org/10.1177/0959683608101389.

Crumley, R.L., Hill, D.F., Beamer, J.P., Holzenthal, E.R., 2019. Seasonal components of freshwater runoff in Glacier Bay, Alaska: diverse spatial patterns and temporal change. Cryosphere 13 (6), 1597–1619. https://doi.org/10.5194/tc-13-1597-2019.

Dugan, D., Fay, G., Colt, S., 2007. Nature-based Tourism in Southeast Alaska: Results from 2005 and 2006 Field Study. Institute of Social and Economic Research, University of Alaska Anchorage.

Etherington, L.L., Hooge, P.N., Hooge, E.R., 2004. Factors affecting seasonal and regional patterns of surface water oceanographic properties within a fjord estuarine system: glacier Bay, Alaska. Anchorage (AK): US Geological Survey, Alaska Science Center.

Etherington, L.L., Hooge, P.N., Hooge, E.R., Hill, D.F., 2007. Oceanography of Glacier Bay, Alaska: implications for biological patterns in a glacial fjord estuary. Estuar. Coast 30, 927–944. https://doi.org/10.1007/BF02841386.

Gabriele, C.M., Amundson, C.L., Neilson, J.L., Straley, J.M., Baker, C.S., Danielson, S.L., 2022. Sharp decline in humpback whale (Megaptera novaeangliae) survival and reproductive success in southeastern Alaska during and after the 2014–2016 Northeast Pacific marine heatwave. Mamm. Biol. 102 (4), 1113–1131. https://doi.org/10.1007/s42991-021-00187-2.

Goldstein, E.D., Pirtle, J.L., Duffy-Anderson, J.T., Stockhausen, W.T., Zimmermann, M., Wilson, M.T., Mordy, C.W., 2020. Eddy retention and seafloor terrain facilitate cross-shelf transport and delivery of fish larvae to suitable nursery habitats. Limnol. Oceanogr. 65 (11), 2800–2818. https://doi.org/10.1002/lno.11553.

Hall, D.K., Benson, C.S., Field, W.O., 1995. Changes of glaciers in Glacier Bay, Alaska, using ground and satellite measurements. Phys. Geogr. 16 (1), 27–41. https://doi.org/10.1080/02723646.1995.10642541.

Halverson, M.J., 2014. Atmospheric and tidal forcing of the exchange between prince William Sound and the Gulf of Alaska. Dynam. Atmos. Oceans 65, 86–106. https://doi.org/10.1016/j.dynatmoce.2013.12.001.

Hersbach, H., Bell, B., Berrisford, P., Biavati, G., Horanyi, A., Munoz Sabater, J., Nicolas, J., Peubey, C., Radu, R., Rozum, I., Schepers, D., Simmons, A., Soci, C., Dee, D., Thepaut, J-N., 2018. ERA5 hourly data on single levels from 1940 to present. Copernicus Climate Change Service (C3S) Climate Data Store (CDS). doi: 10.24381/cds.adbb2d47.

Hill, D.F., Ciavola, S.J., Etherington, L., Klaar, M.J., 2009. Estimation of freshwater runoff into Glacier Bay, Alaska and incorporation into a tidal circulation model. Estuar. Coast Shelf Sci. 82 (1), 95–107. https://doi.org/10.1016/j.ecss.2008.12.019.

Hooge, P.N., Hooge, E.R., 2002. Fjord oceanographic processes in Glacier Bay, Alaska. Glacier Bay Field Station 1–148. USGS-Alaska Science Center. https://www.engr.psu.edu/ce/hydro/hill/research/glba/reports/Hooge_2002_OceanReport.pdf.

Ladd, C., Cheng, W., 2016. Gap winds and their effects on regional oceanography Part I: cross Sound, Alaska. Deep sea res. Part II: topical stud. Oceanography 132, 41–53. https://doi.org/10.1016/j.dsr2.2015.08.006.

Loescher, K.A., Young, G.S., Colle, B.A., Winstead, N.S., 2006. Climatology of barrier jets along the Alaskan coast. Part I: spatial and temporal distributions. Mon. Weather Rev. 134 (2), 437–453. https://doi.org/10.1175/MWR3037.1.

Park, W., Sturdevant, M., Orsi, J., Wertheimer, A., Fergusson, E., Heard, W., Shirley, T., 2004. Interannual abundance patterns of copepods during an ENSO event in Icy Strait, southeastern Alaska. ICES J. Mar. Sci. 61 (4), 464–477. https://doi.org/10.1016/j.icesjms.2004.03.017.

Pawlowicz, R., Beardsley, B., Lentz, S., 2002. Classical tidal harmonic analysis including error estimates in MATLAB using T_TIDE. Comput. Geosci. 28 (8), 929–937. https://doi.org/10.1016/S0098-3004(02)00013-4.

Reed, R.K., Stabeno, P.J., 1993. The recent return of the alaskan stream to near strait. J. Mar. Res. 51 (3), 515–527.

Schumacher, J.D., Stabeno, P.J., Roach, A.T., 1989. Volume transport in the Alaska coastal current. Continent. Shelf Res. 9 (12), 1071–1083. https://doi.org/10.1016/0278-4343(89)90059-9.

Stabeno, P.J., Bell, S., Cheng, W., Danielson, S., Kachel, N.B., Mordy, C.W., 2016a. Long-term observations of Alaska coastal current in the northern Gulf of Alaska. Deep sea res. Part II: topical stud. Oceanography 132, 24–40. https://doi.org/10.1016/j.dsr2.2015.12.016.

Stabeno, P.J., Bond, N.A., Kachel, N.B., Ladd, C., Mordy, C.W., Strom, S.L., 2016b. Southeast alaskan shelf from southern tip of Baranof island to Kayak island: currents, mixing and chlorophyll-a. Deep sea res. Part II: topical stud. Oceanography 132, 6–23. https://doi.org/10.1016/j.dsr2.2015.06.018.

Stabeno, P.J., Bond, N.A., Hermann, A.J., Kachel, N.B., Mordy, C.W., Overland, J.E., 2004. Meteorology and oceanography of the northern Gulf of Alaska. Continent. Shelf Res. 24, 859–897. https://doi.org/10.1016/j.csr.2004.02.007.

Stabeno, P.J., Kachel, D.G., Kachel, N.B., Sullivan, M.E., 2005. Observations from moorings in the aleutian passes: temperature, salinity and transport. Fish. Oceanogr. 14 (Suppl. 1), 39–54. https://doi.org/10.1111/j.1365-2419.2005.00362.x.

Stabeno, P.J., Reed, R.K., Schumacher, J.D., 1995. The Alaska Coastal Current: continuity of transport and forcing. J. Geophys. Res.: Oceans 100 (C2), 2477–2485. https://doi.org/10.1029/94JC02842.

Thomson, R.E., Emery, W.J., 2014. Data Analysis Methods in Physical Oceanography, third ed. Elsevier. https://doi.org/10.1016/B978-0-12-387782-6.01001-2.

Weingartner, T., Eisner, L., Eckert, G.L., Danielson, S., 2009. Southeast Alaska: oceanographic habitats and linkages. J. Biogeogr. 36 (3), 387–400. https://doi.org/10.1111/j.1365-2699.2008.01994.x.

Waite, J.N., Mueter, F.J., 2013. Spatial and temporal variability of chlorophyll-a concentrations in the coastal Gulf of Alaska, 1998–2011, using cloud-free reconstructions of SeaWiFS and MODIS-Aqua data. Prog. Oceanogr. 116, 179–192. https://doi.org/10.1016/j.pocean.2013.07.006.

Zimmermann, M., Benson, J.L., 2013. Smooth sheets: how to work with them in a GIS to derive bathymetry, features and substrates. U.S. Dep. Commer., NOAA Tech. Memo. NMFS-AFSC-249 52.